Mutation in sodium–calcium exchanger 1 (NCX1) causes cardiac fibrillation in zebrafish

Adam D. Langenbacher*†, Yuan Dong*†, Xiaodong Shu*, Jayoung Choi*, Debora A. Nicoll‡§, Joshua I. Goldhaber‡§, Kenneth D. Philipson‡§, and Jau-Nian Chen*‡¶‖**

*Department of Molecular, Cell, and Developmental Biology, ¶Jonsson Comprehensive Cancer Center, ‖Molecular Biology Institute, ‡Cardiovascular Research Laboratory, and §Departments of Physiology and Medicine, University of California, Los Angeles, CA 90095

Edited by Eric N. Olson, University of Texas Southwestern Medical Center, Dallas, TX, and approved October 10, 2005 (received for review March 31, 2005)

Cardiac fibrillation, a form of cardiac arrhythmia, is the most common cause of embolic stroke and death associated with heart failure. The molecular mechanisms underlying cardiac fibrillation are largely unknown. Here we report a zebrafish model for cardiac fibrillation. The hearts of zebrafish *tremblor* (*tre*) mutants exhibit chaotic movements and fail to develop synchronized contractions. Calcium imaging showed that normal calcium transients are absent in *tre* cardiomyocytes, and molecular cloning of the *tre* mutation revealed that the *tre* locus encodes the zebrafish cardiac-specific sodium–calcium exchanger (NCX) 1, NCX1h. Forced expression of NCX1h or other calcium-handling molecules restored synchronized heartbeats in *tre* mutant embryos in a dosage-dependent manner, demonstrating the critical role of calcium homeostasis in maintaining embryonic cardiac function. By creating mosaic zebrafish embryos, we showed that sporadic NCX1h-null cells were not sufficient to disrupt normal cardiac function, but clustered wild-type cardiomyocytes contract in unison in *tre* mutant hearts. These data signify the essential role of calcium homeostasis and NCX1h in establishing rhythmic contraction in the embryonic zebrafish heart.

calcium homeostasis | cardiac arrhythmia | heart

The heart is a muscular pump that drives circulation throughout the body. It is of the utmost importance to establish rhythmic and synchronized cardiac contraction early in development to ensure proper growth and survival of the embryo.

Calcium plays an essential role in regulating cardiac cycles. As a wave of depolarization passes through the heart, a small amount of calcium is permitted to enter the cardiomyocytes through voltage-dependent L-type calcium channels. This small calcium influx then triggers the release of a larger amount of calcium from the sarcoplasmic reticulum via ryanodine receptors, resulting in an abrupt increase in cytosolic calcium levels and cardiac contraction. Relaxation is accomplished by resequestering of calcium to the sarcoplasmic reticulum by sarcoendoplasmic reticular Ca^{2+}-ATPase2 (SERCA2) and extrusion of calcium from the cell by NCX1 and plasma membrane Ca^{2+}-ATPase (PMCA). Abnormal calcium handling caused by altered expression levels or protein activities of NCX1 and SERCA2, or by mutations in ryanodine receptors, have been associated with cardiac diseases, such as heart failure and arrhythmia, and with sudden death in humans and animal models (1–6). In addition, genetic studies in the zebrafish demonstrate that L-type calcium channels and the sodium pump (a modulator of NCX activity) are indispensable for embryonic cardiac function (7, 8). These findings underscore the critical roles of calcium in embryonic and adult cardiac physiology.

Three NCX genes have been identified in mammals. NCX2 and NCX3 are expressed predominantly in the brain and skeletal muscle, respectively, whereas NCX1 is virtually ubiquitous (9). NCX1 is highly expressed in the heart and is considered to be the primary mechanism for calcium extrusion in cardiomyocytes. In fact, elevated NCX1 activity has been noted in patients with heart failure and is associated with arrhythmia in patients and animal models (1, 2). The embryonic role of NCX1, however, is not well understood. Whereas NCX1−/− embryos exhibit severe cardiac defects ranging from arrhythmia to weak cardiac contraction and a silent heart (10–13), the MLC2v-Cre-driven cardiac-specific NCX1 knockout mice survive to adulthood (14), raising a debate about whether the activity of NCX1 is dispensable in the developing heart. The investigation of the requirement of NCX1 in heart development is further complicated by severe placental vascular defects and early embryonic lethality (10–13). An additional genetic model is required to elucidate the role of NCX1 in the developing heart.

Here we report the identification of two zebrafish NCX1 homologues, NCX1n and NCX1h. *In situ* hybridization analysis showed that these genes have distinct expression patterns. NCX1n is predominantly expressed in the brain and neural tube, whereas NCX1h is cardiac-specific. By a morpholino knockdown assay and positional cloning of the zebrafish *tremblor* (*tre*) locus, we show that NCX1h activity is required for maintaining rhythmicity and calcium transients in the embryonic zebrafish heart. Forced expression of wild-type NCX1h or other calcium-handling genes restored synchronized heartbeats in *tre* mutants, indicating that abnormal calcium flux is the cause of the cardiac fibrillation phenotype.

Materials and Methods

Zebrafish Strains and Studies. Zebrafish colonies were cared for and bred as described in ref. 15. Developmental stages of zebrafish embryos were determined by using standard morphological features of fish raised at 28.5°C (16). The *tremblor*^{tc318} allele was obtained from the Tübingen stock center.

Isolation of Zebrafish NCX1 Homologues. Partial sequences of NCX1n and NCX1h were amplified (94°C for 30 sec, 60°C for 60 sec, and 72°C for 60 sec for 32 cycles) and cloned into pCR II-TOPO vector (Invitrogen) by using the following primers: NCX1n forward, AGTGACACTGGTGAGAATGAC; NCX1n reverse, ATGGCTGTCTTCAAAGTCCTC; NCX1h forward, TAGACTTATGACTGGTGCAGG; NCX1h reverse, ACTCCATGGGTGTCTTCAAAG. The full-length sequences of NCX1n and NCX1h were isolated by RACE. Total RNA was isolated from 30 h postfertilization (hpf) wild-type embryos with the RNAqueous-4 PCR kit (Ambion, Austin, TX). RACE was performed with the SMART RACE cDNA amplification kit (BD Biosciences) according to the manufacturer's protocol.

Conflict of interest statement: No conflicts declared.

This paper was submitted directly (Track II) to the PNAS office.

Abbreviations: hpf, hours postfertilization; NCX, sodium–calcium exchanger; PMCA, plasma membrane Ca^{2+}-ATPase; SERCA2, sarcoendoplasmic reticular Ca^{2+}-ATPase; *tre*, *tremblor*.

Data deposition: The sequences reported in this paper have been deposited in the GenBank database [accession nos. AY934775 (NCX1h) and AY934776 (NCX1n)].

†A.D.L. and Y.D. contributed equally to this work.

**To whom correspondence should be addressed at: Department of Molecular, Cell, and Developmental Biology, University of California, 621 Charles E. Young Drive South, LSB 5109, Los Angeles, CA 90095. E-mail: chenjn@mcdb.ucla.edu.

GENETICS

Primers used for RACE were as follows: NCX1n 5′RACE, CGGACACGGTTTGATTGAGATCGC; NCX1n 3′RACE, ATCGTCGGCAGTGCAGCTTTCAAC; NCX1h 5′RACE, TGT ACTCCACTGACACAGTGCTGG.

Morpholino Injections. A morpholino antisense oligonucleotide (Gene Tools, Philomath, OR) complementary to the translation start site of NCX1h and its flanking sequence (NCX1hMO, GATGAAGTCCCAGATTGGCCCATGT) was synthesized. At the one- to two-cell stage, 1.5 ng of NCX1hMO was injected into cmlc2::EGFP transgenic embryos (17). Cardiac phenotypes were examined by digital imaging and whole-mount *in situ* hybridization at 24 hpf and 50 hpf.

Genetic Mapping and Positional Cloning. We established the *tre* map cross by mating a male *tre* heterozygote to a female fish from the TL strain. Linkage between *tre* and simple sequence-length polymorphism (SSLP) markers was analyzed as previously described in ref. 18. Total mRNA was extracted from pools of 50 homozygous mutant embryos or 50 of their wild-type siblings (RNAwiz, Ambion) for cDNA synthesis (Access RT-PCR system, Promega). PCR and RT-PCR products were subcloned by using the TOPO TA cloning kit (Invitrogen) for subsequent sequencing analysis.

Restriction Fragment-Length Polymorphism Analysis. Genomic DNA of *tre* mutants and their wild-type siblings were individually prepared and amplified by two pairs of nested primers flanking the *tre* mutation (F1, TTCTCACAGGGTACTGGAGAG; R1, CAAAATGCCAAACACTCTTCATAG; F2, GCCACTAGA CTTATGACTGGTGC; R2, CTAAAGCGTCCACATGATT-GGT). The PCR products were digested with MseI overnight at 37°C and analyzed on a 2% agarose gel.

Phenotypic Rescue. Capped mRNA for PMCA, SERCA2 (purchased from Open Biosystems, Huntsville, AL), canine NCX1, wild-type NCX1h, and tre^{tc318} NCX1h was synthesized by *in vitro* transcription with the mMESSAGE mMACHINE kit (Ambion). These mRNAs were injected into one- to two-cell stage embryos from a cross of *tre* heterozygotes. Cardiac phenotypes of the injected embryos were examined by digital imaging at 30 hpf and 50 hpf. All injected embryos were genotyped by MseI restriction fragment-length polymorphism analysis.

Calcium Imaging. Embryos from crosses of *tre* heterozygotes were injected with 1 nl of a 250 μM stock of calcium green-1 dextran (Molecular Probes) at the one-cell stage. Hearts of 2-day-old *tre* mutants and their wild-type siblings were dissected out and placed in Tyrode's solution supplemented with 0.0018 g/ml glucose. High-speed two-dimensional calcium images were captured at a rate of 30 Hz by a Noran Odyssey XL laser scanning confocal imaging system using a ×40 objective lens, excitation at 488 nm, and emission at 510 nm. The fluorescence intensity of individual hearts was analyzed by INTERVISIA software.

Sodium Gradient-Dependent Calcium Uptake Assay. The coding sequences of wild-type and the tre^{tc318} mutant form of NCX1h were subcloned into the pCS2+ vector under the control of the CMV promoter and transfected into HEK293 cells with GenePORTER (Gene Therapy System, San Diego). Cells were harvested for NCX uptake assays 48 h after transfection as previously described in ref. 19. In brief, cells were washed twice and loaded with Na^+ by incubating with 10 mM Mops (pH 7.4), 140 mM NaCl, 1 mM $MgCl_2$, 0.4 mM ouabain, and 25 μM nystatin for 10 min at room temperature. Uptake was initiated by resuspending the cell pellet in 10 mM Mops (pH 7.4), 140 mM KCl (or NaCl as control), 25 μM $CaCl_2$, 0.4 mM ouabain, and 5 μCi/ml (1 Ci = 37 GBq) $^{45}Ca^{2+}$ for 1 min. The reaction was stopped by adding 1 ml of quenching solution (140 mM KCl/1 mM EGTA) followed by two additional washes with the quenching solution. Cell pellets were then dissolved in 1 M NaOH at 80°C for 20 min and subjected to scintillation counting and normalized to total cellular protein. The protein concentration was measured by micro bicinchoninic acid (Pierce) with BSA as standards.

***In Situ* Hybridization.** Embryos for *in situ* hybridization were raised in embryo medium supplemented with 0.2 mM 1-phenyl-2-thiourea to maintain optical transparency (15). Whole-mount *in situ* hybridization was performed as described in ref. 20. The antisense RNA probes used in this study were *Pax2* (from F. Serluca, Novartis Institute for Biomedical Research), *cmlc2*, *vmhc*, *versican* (from D. Y. Stainier, University of California, San Francisco), *SERCA2* (Open Biosystems), *flk1/VEGFR2* (21), *Nkx2.5* (20), *Irx1* (8), *NCX1n*, and *NCX1h.*

Histology. Fixed embryos were dehydrated, embedded in plastic (JB-4, Polysciences), sectioned at 8 μm, and stained with 0.1% methylene blue as previously described in ref. 20.

Transplantation. Transplantation procedures were previously described in ref. 20. In brief, embryos used for transplantation experiments were collected from the intercross of tre^{tc318} heterozygotes. Thus, 25% of these embryos will show a fibrillation phenotype, whereas the other 75% are phenotypically wild-type. Embryos used as donors were injected with 1 nl of 5% tetramethylrhodamine dextran at the one-cell stage. At the early blastula stage, ≈20 blastomeres were retrieved from the donors and transplanted to the margin of uninjected siblings (recipients). After 48 h of development, embryos were inspected with fluorescence microscopy for coordinated cardiac contraction.

Results and Discussion

To investigate the role of NCX1 in embryonic heart development in the zebrafish, we used mouse NCX1 sequence to perform a BLAST search of the zebrafish Ensembl database, available through the Sanger Institute, and identified two NCX1 homologues. The full-length coding sequences of these genes were then obtained by 5′ and 3′ RACE RT-PCR. Both genes encode proteins with a high degree of identity to mammalian NCX1 proteins (Fig. 1 *A* and *B*) and are likely to be paralogues arisen from the teleost genome duplication (22). *In situ* hybridization analysis revealed that these zebrafish NCX1 genes have distinct expression patterns (see below). Based on their expression patterns, we named the gene on chromosome 11 "NCX1h" and the gene on chromosome 17 "NCX1n."

NCX1n transcripts are evident throughout the developing embryo at low levels during somitogenesis and become restricted to the neural tissues and fin buds in 2-day-old embryos (Fig. 1 *C–E*). Whereas NCX1n transcripts are not detected in the heart (Fig. 1*E*), NCX1h is cardiac-specific. NCX1h expression is detected in the bilateral cardiac primordia during somitogenesis and throughout the primitive heart tube by 24 hpf (Fig. 1 *F* and *G*). After 2 days of development, NCX1h transcripts are found prominently in myocardium of the atrium and ventricle and are barely detectable in the outflow tract (Fig. 1*H*). Interestingly, the combined expression patterns of zebrafish NCX1n and NCX1h are comparable to the expression pattern of mammalian NCX1 (23), suggesting that each of these paralogues assumes part of the function of the ancestral NCX1 by subfunctionalization of duplicated genes (22). The distinct expression patterns of NCX1n and NCX1h also suggest that they are involved in different biological processes and that NCX1h has a role in embryonic heart development.

We analyzed the potential roles of NCX1h in zebrafish heart development using a knockdown approach. We designed a

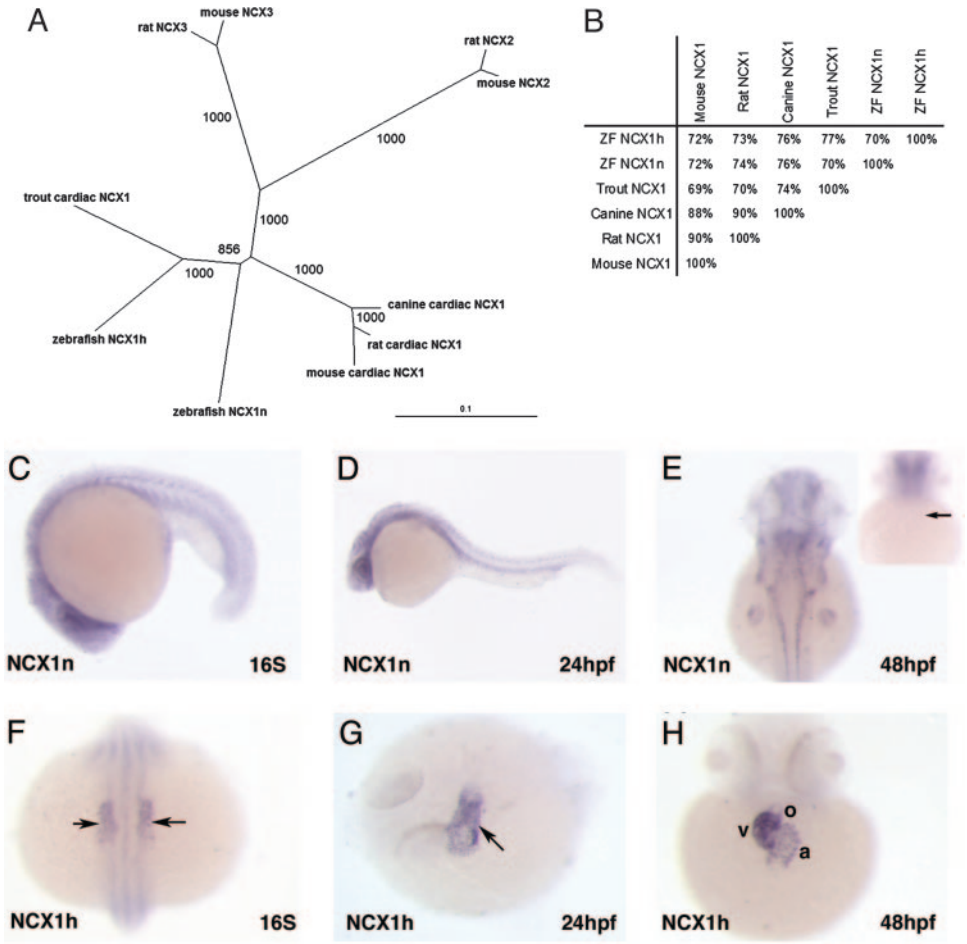

Fig. 1. Zebrafish NCX1 homologues. (*A*) Phylogeny of NCX homologues in rat, mouse, canine, trout, and zebrafish. The tree was calculated in CLUSTALX by using the neighbor-joining method. Numbers at branches are bootstrap values. The unit of the scale represents amino acid substitutions per site. (*B*) Both NCX1n and NCX1h share high identity to other NCX1 proteins throughout the entire peptide. (*C–E*) *In situ* hybridization analysis showed that NCX1n is expressed throughout the zebrafish embryo at 16S (*C*) and becomes more strongly expressed in the brain and the neural tube at 24 hpf (*D*). By 48 hpf, NCX1n expression is restricted to the brain, the neural tube, and the fin bud, but not in the heart (*E*). *Inset* in *E* shows the ventral view focusing on the heart. The arrow points to the heart. (*F–H*) NCX1h is a cardiac-specific gene. NCX1h is expressed in cardiac precursors at 16S (*F*). At 24 hpf, the transcripts of NCX1h are detected throughout the primitive heart tube (*G*). By 48 hpf, NCX1h transcripts are found prominently in the myocardium of the atrium and ventricle and are barely detectable in the outflow tract (*H*). a, atrium; v, ventricle; o, outflow tract. Arrows point to the heart.

morpholino antisense oligonucleotide specifically targeting the translation initiation site of NCX1h (NCX1hMO) and found that injecting 1.5 ng of NCX1hMO into wild-type zebrafish embryos did not affect the patterning of the primitive heart tube but was sufficient to disrupt synchronized cardiac contraction (99%, n = 421). The uncoordinated heartbeat became even more pronounced in 2-day-old NCX1h morphants (referring to embryos injected with NCX1hMO) where the cardiomyoctyes developed a chaotic movement resembling a condition known as fibrillation in humans. We also noted that, although cardiac fibrillation was observed in both chambers, the chaotic movement was more pronounced in the atrium than in the ventricle. This phenotype is similar to that observed in *tre* mutants (24, 25), raising the possibility that the *tre* locus encodes NCX1h (see Movies 1–4, which are published as supporting information on the PNAS web site).

We investigated whether NCX1h is linked to the *tre* locus using Z4190, a genetic marker near NCX1h (http://zebrafish.mgh.harvard.edu). We detected only 10 recombinations between Z4190 and the *tre* locus from 310 meiosis, indicating that Z4190 was linked to *tre*. Sequencing analysis revealed a G to T transversion in *tre*^{tc318} mutants at codon 489 of NCX1h, creating a premature stop codon and a MseI restriction enzyme site (Fig. 2 *A* and *B*). We found that this MseI restriction fragment-length polymorphism cosegregated with an additional 163 individual *tre* mutant embryos, further indicating that NCX1h is encoded by the *tre* locus. The truncated tre^{tc318} protein lacks most of the intracellular loop and the four C-terminal transmembrane domains, which are essential for calcium binding and transport (26), and is, therefore, likely to be nonfunctional. We tested the calcium-transporting activity of tre^{tc318} in HEK cells. Lysates of HEK cells transfected with wild-type NCX1h and *tre*^{tc318} were normalized based on the levels of total cellular protein before being subjected to the sodium-gradient-dependent calcium uptake analysis. As shown in Fig. 2*C*, HEK cells transfected with *tre*^{tc318} have the endogenous basal level of transporting activity, supporting the notion that *tre*^{tc318} is a null allele.

To analyze whether overexpression of NCX1h is capable of rescuing cardiac fibrillation in *tre*, we injected NCX1h mRNA into wild-type and *tre* mutant embryos. Forced expression of NCX1h in wild-type embryos did not cause obvious morphological or functional defects (n = 179 for 100-pg injection, and n = 265 for 150-pg injection), consistent with the finding that transgenic mice overexpressing NCX1 develop relatively nor-

GENETICS

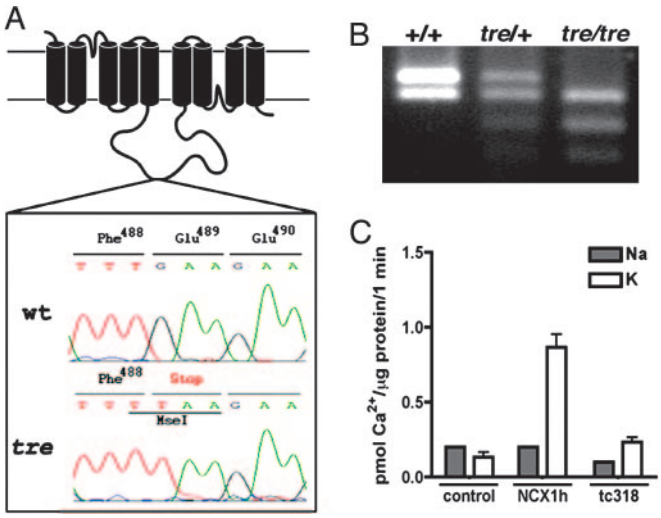

Fig. 2. The *tre* locus encodes NCX1h. (*A*) Schematic diagram of NCX1h protein. A G to T transversion at codon 489 is detected in tre^{tc318}, which creates a premature stop codon and MseI polymorphism. (*B*) MseI restriction fragment-length polymorphism in wild type, *tre* heterozygotes, and *tre* homozygotes. (*C*) Na^+ gradient-dependent uptake assay. HEK293 cells transfected with zebrafish NCX1h (NCX1h) showed significant $^{45}Ca^{2+}$ uptake in the presence of an outwardly directed Na^+ gradient. $^{45}Ca^{2+}$ uptake in cells transfected with tre^{tc318} (tc318) remained at basal levels similar to the vector transfected cells (control). The gray bars represent uptake activities in the absence of a Na^+ gradient, and the white bars represent uptake in the presence of an outwardly directed Na^+ gradient.

mally (27). Overexpression of NCX1h was, however, able to rescue the *tre* fibrillation phenotype in a dosage-dependent manner. Whereas 64% of the 100-pg NCX1h mRNA-injected *tre* mutant embryos manifested weak but synchronized heartbeats, 91% of 150-pg NCX1h mRNA-injected *tre* mutants had coordinated heartbeats (Table 1). These data demonstrate that forced expression of NCX1h is sufficient to restore coordinated cardiac contraction in a *tre* mutant background and support the notion that loss of function of NCX1h is the cause of cardiac fibrillation in *tre*. Furthermore, the sequence of NCX1 is highly conserved among species (26). We tested whether mammalian NCX1 could rescue *tre* fibrillation phenotype and found that canine NCX1 could indeed restore synchronized heartbeat in *tre* (Table 1; see also Movies 5 and 6, which are published as supporting information on the PNAS web site), indicating that the function, as well as the sequence, of NCX1 is well conserved from zebrafish to mammals.

The primary role of NCX is calcium extrusion. The truncated protein produced by the tre^{tc318} mutation may result in abnormal calcium fluxes. To monitor calcium transients *in vivo*, we injected calcium green-1 dextran into wild-type and *tre* mutant embryos at the one-cell stage, so that as the cells divided the calcium indicator would be distributed to all embryonic cells. By visual inspection, we found that calcium signals appeared to fluctuate as the heart contracted in wild-type embryos but remain at a relatively constant level in *tre* mutants (Fig. 3*A*). We used high-speed two-dimensional confocal calcium imaging to analyze calcium transients in wild-type and *tre* mutant hearts. We detected a wave of calcium-induced fluorescence traveling across the wild-type heart with each heartbeat but only chaotic and unsynchronized fluorescence signals in individual *tre* cardiomyocytes and in the heart of NCX1h morphants (Fig. 3 *B–D*; see also Movies 7–9, which are published as supporting information on the PNAS web site). These data demonstrate abnormal calcium transients in the hearts of *tre* and NCX1h morphants, which might be the cause of their cardiac fibrillation phenotypes. If abnormal calcium homeostasis was indeed the cellular mechanism underlying the *tre* fibrillation phenotype, we hypothesized that enhancing activities of other calcium-handling proteins might compensate for the tre^{tc318} defect. To test this hypothesis, we injected PMCA and SERCA2 mRNA, two molecules involved in removing cytosolic calcium, into *tre* mutants and found that they could restore synchronized cardiac contraction in *tre* (Table 1), supporting the notion that an imbalance in calcium homeostasis is the cause of cardiac fibrillation in *tre* mutants. Interestingly, upon more careful analysis, we noted that, even though the *tre* fibrillation phenotype could be suppressed by overexpression of SERCA2, the SERCA2-rescued *tre* heart does not dilate as much as the PMCA-, canine NCX1-, or zebrafish NCX1h-rescued *tre* heart (see Movies 6 and 10, which are published as supporting information on the PNAS web site). Whether this phenotype reflects the different roles of SERCA2 and PMCA and NCX1 in calcium handling and whether overexpression of these proteins induces other secondary physiological responses requires further investigation.

Our data demonstrate that the NCX1h-null heart fibrillates. To investigate whether a few NCX1h-null cells are sufficient to disrupt synchronized contractions of an otherwise normal heart, we created mosaic embryos by transplanting *tre* blastomeres into wild-type embryos. We obtained 10 chimeric embryos that had 20–50 *tre* mutant cells sporadically distributed in the hearts. The contraction pattern of these chimeric hearts was similar to

Table 1. Summary of RNA rescue of *tre* fibrillation phenotype

RNA injected	No. of *tre* embryos	No. of *tre* embryos with coordinated heartbeat	No. of *tre* embryos with fibrillation	% of *tre* embryos with coordinated heartbeat
Uninjected control	305	23	282	7.5
NCX1h				
100 pg	62	40	22	64
150 pg	87	79	8	91
Canine NCX1				
50 pg	96	25	71	26
75 pg	109	67	42	61
100 pg	92	61	31	66
PMCA				
150 pg	59	29	30	49
200 pg	70	49	21	70
SERCA2				
200 pg	81	50	31	62

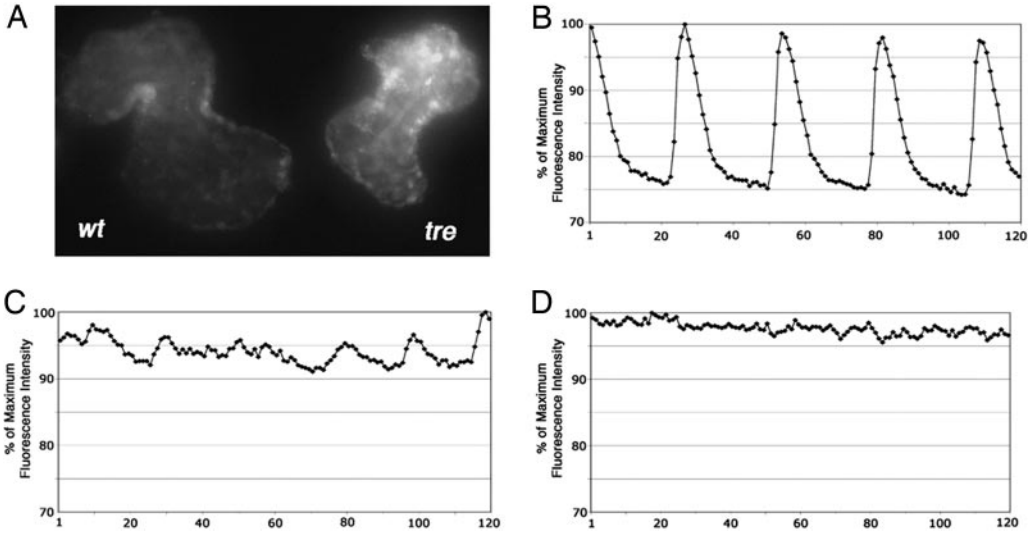

Fig. 3. Calcium imaging. (*A*) The fluorescent signals of calcium green dextran are detected in 2-day-old wild-type heart (*Left*) and *tre* mutant heart (*Right*). (*B–D*) High-speed two-dimensional confocal imaging shows transients of elevated calcium levels in the wild-type heart (*B*) but only unsynchronized calcium fluctuations in the *tre* mutant (*C*) and NCX1h morphant heart (*D*). Data were collected at 30 frames per sec. The relative fluorescence intensities (*y* axis) from consecutive frames of images (*x* axis) are plotted in graphs, where the maximum fluorescence intensity of each data set is considered to be 100%.

normal hearts (see Fig. 5*A* and Movie 11, which are published as supporting information on the PNAS web site), suggesting that waves of depolarization can bypass a small number of NCX1h-null cells and continue traveling through the developing zebrafish heart. In a reversed transplantation experiment, we obtained *tre* mutant embryos that hosted wild-type cardiomyocytes. Interestingly, the wild-type donor cells tended to form clusters, rather than to evenly distribute, in *tre* hearts. Of the nine chimera we analyzed, all had clusters of wild-type cells (10–20 cells in each cluster). These clustered wild-type cardiomyocytes

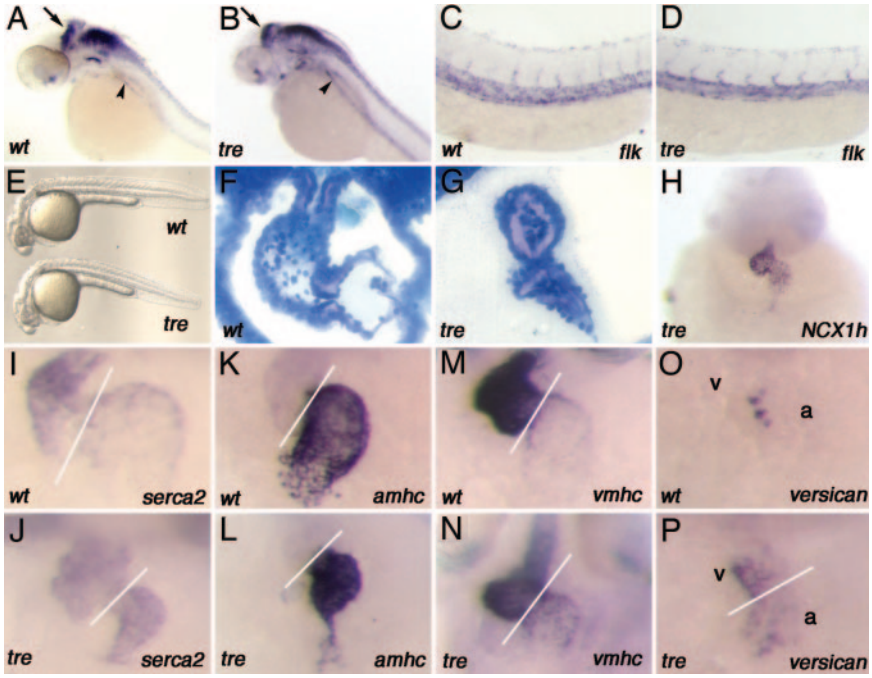

Fig. 4. Loss of function phenotypes of NCX1h. The NCX1h defect is cardiac-specific. (*A–E*) *In situ* hybridization with *pax2* (*A* and *B*) and *flk1* (*C* and *D*) probes show that the development of the brain, kidney, and vasculature are not affected in *tre*, and the overall morphologies of *tre* (*Lower*) is similar to wild-type embryos (*Upper*) at 24 hpf (*E*). The arrows point to the midbrain–hindbrain boundary, and the arrowheads point to the developing pronephric duct in *A* and *B*. (*F* and *G*) Histological sections showed that, whereas a well patterned and dilated atrium and ventricle were observed in the wild-type heart (*F*), the *tre* heart is small, and the posterior end of the atrium collapsed (*G*). (*H*) The expression level of NCX1h is prominent in *tre* mutant heart at 48 hpf. (*I*) The expression of SERCA2 is abundant in the ventricle and present at lower levels in the atrium of 2-day-old wild-type embryos. (*J*) In 2-day-old *tre* mutant hearts, the atrial expression of SERCA2 expression is slightly elevated. The cardiac expression patterns of *amhc* and *vmhc* are restricted to their respective chambers in both wild-type (*K* and *M*) and *tre* (*L* and *N*) embryos. The expression of versican extends to the atrium and ventricle in *tre* mutants (*P*), whereas the expression of this gene is restricted to the boundary of atrium and ventricle in wild-type embryos after 2 days of development (*O*). Lines mark the boundary of atrium and ventricle. a, atrium; v, ventricle.

GENETICS

contracted as a unit in the otherwise fibrillating heart (Fig. 5*B*; see also Movie 12, which is published as supporting information on the PNAS web site), demonstrating that, in the *tre* fibrillation background, wild-type cells can couple with each other.

The effect of NCX1h appears to be cardiac-specific in zebrafish. The overall morphology of the embryos and the formation of the brain, kidney (analyzed by *pax2*), and vasculature (analyzed by *flk1*) are unaffected in 1-day-old *tre* mutants (Fig. 4 *A–E*). After 2 days of development, a prominent cardiac edema is noted in *tre*, and the morphology of the 2-day-old *tre* heart is also affected. The posterior end of the atrium collapses, the ventricle fails to fully dilate, and the space between the myocardium and endocardium becomes significantly wider in *tre* than is observed in wild-type siblings (Fig. 4 *F* and *G*). Transcripts derived from null mutations are usually nondetectable or are significantly reduced in mutant embryos. In 2-day-old *tre* mutant hearts, we detected significant levels of NCX1h transcripts (Fig. 4*H*), indicating that nonsense-mediated decay does not have a great impact on tre^{tc318} mRNA. The expression level of SERCA2 is slightly elevated in the atrium of *tre*, implying a potential compensation effect (Fig. 4 *I* and *J*). Furthermore, whereas the expression patterns of many cardiac chamber-specific genes, including *irx1* (not shown), *amhc*, and *vmhc,* are normal (Fig. 4 *K–N*), the expressions of *versican* (Fig. 4 *O* and *P*) and *bmp4* (not shown) fail to be confined to the chamber boundaries and spread through both cardiac chambers in *tre* mutants. These data signify that the cardiac chamber-specific differentiation program has been initiated, but the differentiation is either incomplete or not being maintained properly in *tre* mutant hearts. These data also demonstrate that the activity of NCX1h is required for proper cardiac morphogenesis. However, because the cardiac fibrillation phenotype is evident in 1-day-old *tre* embryos, it is a formal possibility that the abnormal cardiac morphogenesis is secondary to the fibrillation defect.

The mechanisms underlying cardiac fibrillation are largely unknown. It is believed that a functional defect or an anatomical obstacle caused by cardiac infarction, ischemia, or fibrosis may break electrical waves and cause cardiac fibrillation (28). Our study on the zebrafish *tre/NCX1h* mutation provides genetic and cellular evidence that intrinsic cellular properties, such as calcium homeostasis, are important factors for cardiac fibrillation. We show that failure in calcium extrusion by loss of function of NCX1h disrupts normal calcium transients and causes cardiac fibrillation in the zebrafish. We propose as a model that loss of function of NCX1h causes an imbalance of cytosolic calcium in cardiomyocytes, which then triggers spontaneous calcium release from the sarcoplasmic reticulum independent of the stimulation of membrane depolarization and leads to cardiac fibrillation in *tre* mutants. This model is consistent with "triggered arrhythmia" caused by early and delayed afterdepolarization (29).

In mammals, NCX1 is expressed in a broad range of tissues (9), and the secondary effects of noncardiac defects and early embryonic lethality have made the assessment of the role of NCX1 in the developing heart difficult (10–13). Our finding that zebrafish NCX1h is a cardiac-specific gene provides a genetic model to analyze the primary effect of NCX1 on heart development, and the fact that zebrafish embryos can survive without a functioning heart (30) offers an opportunity to inspect cardiac phenotypes as the disease develops *in vivo*. Because the function of NCX1 is conserved from fish to mammals, studies carried out in the fish model will be complementary to the existing mammalian models. Furthermore, by using the mutagenized zebrafish, hundreds of mutants with cardiac defects have been identified (24, 25, 31). Some of these mutants are defective in calcium-handling proteins, such as the L-type calcium channel and Na,K-ATPase (7, 8). These mutants, together with *tre/NCX1h*, will facilitate studies on gene functions and gene interactions at the genetic, organismic, and cellular physiology levels.

We thank Y. B. Wang and members of the J.-N.C. laboratory for discussion and F. Laski for critical comments on the manuscript. This work was supported by National Institutes of Health Grants HL48509 (to K.D.P.) and HD41367 (to J.-N.C.) and the Laubisch Foundation (J.-N.C.).

1. Pogwizd, S., Qi, M., Yuan, W., Samarel, A. & Bers, D. (1999) *Circ. Res.* **85,** 1009–1019.
2. Pogwizd, S. & Bers, D. (2002) *Ann. N.Y. Acad. Sci.* **976,** 454–465.
3. Frank, K., Bolck, B., Erdmann, E. & Schwinger, R. (2003) *Cardiovasc. Res.* **57,** 20–27.
4. Priori, S., Napolitano, C., Tiso, N., Memmi, M., Vignati, G., Bloise, R., Sorrentino, V. & Danieli, G. (2001) *Circulation* **103,** 196–200.
5. Laitinen, P., Brown, K., Piippo, K., Swan, H., Devaney, J., Brahmbhatt, B., Donarum, E., Marino, M., Tiso, N., Viitasalo, M., *et al.* (2001) *Circulation* **103,** 485–490.
6. Wehrens, X., Lehnart, S., Huang, F., Vest, J., Reiken, S., Mohler, P., Sun, J., Guatimosim, S., Song, L., Rosemblit, N., *et al.* (2003) *Cell* **113,** 829–840.
7. Rottbauer, W., Baker, K., Wo, Z., Mohideen, M., Cantiello, H. & Fishman, M. (2001) *Dev. Cell* **1,** 265–275.
8. Shu, X., Cheng, K., Patel, N, Chen, F., Joseph, E., Tsai, H. & Chen, J. (2003) *Development* **130,** 6165–6173.
9. Blaustein, M. & Lederer, W. (1999) *Physiol. Rev.* **79,** 763–854.
10. Wakimoto, K., Kobayashi, K., Kuro-o, M., Yao, A., Iwamoto, T., Yanaka, N., Kita, S., Nishida, A., Azuma, S., Toyoda, Y., *et al.* (2000) *J. Biol. Chem.* **275,** 36991–36998.
11. Cho, C.-H., Kim, S. S., Jeong, M. J., Lee, C. O. & Shin, H. S. (2000) *Mol. Cells* **10,** 712–722.
12. Koushik, S. V., Wang, J., Rogers, R., Moskophidis, D., Lambert, N. A., Creazzo, T. L. & Conway, S. J. (2001) *FASEB J.* **15,** 1209–1211.
13. Reuter, H., Henderson, S., Han, T., Ross, R., Goldhaber, J. & Philipson, K. (2002) *Circ. Res.* **90,** 305–308.
14. Henderson, S., Goldhaber, J., So, J., Han, T., Motter, C., Ngo, A., Chantawansri, C., Ritter, M., Friedlander, M., Nicoll, D., *et al.* (2004) *Circ Res.* **95,** 604–611.
15. Westerfield, M. (1995) *The Zebrafish Book* (Univ. of Oregon Press, Eugene).
16. Kimmel, C., Ballard, W., Kimmel, S., Ullmann, B. & Schilling, T. (1995) *Dev. Dyn.* **203,** 253–310.
17. Huang, C., Tu, C., Hsiao, C., Hsieh, F. & Tsai, H. (2003) *Dev. Dyn.* **228,** 30–40.
18. Shimoda, N., Knapik, E., Ziniti, J., Sim, C., Yamada, E., Kaplan, S., Jackson, D., de Sauvage, F., Jacob, H. & Fishman, M. (1999) *Genomics* **28,** 219–232.
19. Qiu, Z., Nicoll, D. & Philipson, K. (2001) *J. Biol. Chem.* **276,** 194–199.
20. Chen, J. & Fishman, M. (1996) *Development* **122,** 3809–3816.
21. Chan, J., Bayliss, P., Wood, J. & Roberts, T. (2002) *Cancer Cell* **1,** 257–267.
22. Force, A., Lynch, M., Pickett, F., Amores, A., Yan, Y. & Postlethwait, J. (1999) *Genetics* **151,** 1531–1545.
23. Koushik, S., Bundy, J. & Conway, S. (1999) *Mech. Dev.* **88,** 119–122.
24. Chen, J., Haffter, P., Odenthal, J., Vogelsang, E., Brand, M., van Eeden, F., Furutani-Seiki, M., Granato, M., Hammerschmidt, M., Heisenberg, C., *et al.* (1996) *Development* **123,** 293–302.
25. Stainier, D., Fouquet, B., Chen, J., Warren, K., Weinstein, B., Meiler, S., Mohideen, M., Neuhauss, S., Solnica-Krezel, L., Schier, A., *et al.* (1996) *Development* **123,** 285–292.
26. Philipson, K. & Nicoll, D. (2003) *Annu. Rev. Physiol.* **62,** 111–133.
27. Reuter, H., Han, T., Motter, C., Philipson, K. & Goldhaber, J. (2003) *J. Physiol.* **5543,** 779–789.
28. Xie, F., Qu, Z., Yang, J., Baher, A., Weiss, J. & Garfinkel, A. (2004) *J. Clin. Invest.* **113,** 686–693.
29. Pogwizd, S. & Bers, D. (2004) *Trends Cardiovasc. Med.* **14,** 61–66.
30. Chen, J. & Fishman, M. (2000) *Trends Genet.* **16,** 383–388.
31. Alexander, J., Stainier, D. & Yelon, D. (1998) *Dev. Genet.* **22,** 288–299.